

Phase formation and crystallization kinetics of CuIn_5S_8 amorphous films

© G.E. Dashdamirova¹, E.B. Askerov^{2,3}, D.I. Ismailov¹

¹ Institute of Physics, National Academy of Science, AZ1143 Baku, Azerbaijan

² Joint Institute for Nuclear Research, 141980 Dubna, Moscow oblast, Russia

³ National Nuclear Research Center, 370143 Baku, Azerbaijan

E-mail: elmar.asgerov@gmail.com

Received November 17, 2021

Revised November 25, 2021

Accepted November 25, 2021

The processes of interaction and formation of phases in the Cu_2S – In_2S_3 system obtained by sequential and simultaneous deposition of Cu_2S and In_2S_3 binary compounds in vacuum have been investigated. Using the kinematic electron diffraction method, the kinetic crystallization parameters of CuIn_5S_8 amorphous films formed as a result of vacuum condensation of the above binary compounds, both under normal conditions and under the influence of an external electric field, have been established.

Keywords: kinematic electron diffraction, nanosized films, condensation plane.

DOI: 10.21883/SC.2022.03.53060.9773

1. Introduction

CuIn_5S_8 ternary compound semiconductor is classified as $\text{M B}_5^{\text{III}}\text{C}_8^{\text{VI}}$ (M — Cu, Fe, Mn; B^{III} — In, Ga, Al; C^{VI} — S, Se, Te) type semiconductors. CuIn_5S_8 has ordered defects with concentration $\sim 25\%$. The study [1] describes the prospects of this compound for creation of high-efficiency solar cells — wide-band natural emission converters, because its photosensitivity at $T = 300\text{ K}$ is changed within 1.2–3.5 eV. The best range of values for solar energy conversion is 1.2–1.4 eV. In accordance with [2–4], CuIn_5S_8 compound together with effective optical emitters may be also used as a material for creation of various types of infrared detectors and heterojunctions. The Cu–S system has three individual stable phases: Cu_9S_5 (digenite), CuS (covellite) and Cu_2S (chalcocite) with a density of $\rho = 5.8\text{ g/cm}^3$. Chalcocite has two modifications: low-temperature and high-temperature ones [5]. According to [5], low-temperature Cu_2S belongs to $Ab2m(C_{2v}^{15})$ space symmetry group (SSG) and has a rhombic cell with $a = 11.90$, $b = 27.28$, $c = 13.41\text{ \AA}$. Constants of hexagonal lattices with SSG C_6/mmc of high-temperature chalcocite existing at $> 378\text{ K}$ are equal to: $a = 3.89$, $c = 6.68\text{ \AA}$.

Thermodynamic analysis of the In–S system in [5] found four sulfides: InS, In_5S_6 , In_3S_4 and In_2S_3 that are congruently melting at 1363 K. In_2S_3 compound, together with Cu_2S , is dimorphous and has low-temperature and high-temperature α and β phases, respectively. Higher than 573 K, α -modification irreversibly moves into a high-temperature β -modification with a spinel type structure. According to [5], crystallographic constants α - In_2S_3 have a face-centered cubic lattice with $a = 5.37\text{ \AA}$, SSG

$Fd3m-O_h^7$, X-ray density $\rho = 4.9\text{ g/cm}^3$. A CuIn_5S_8 compound is crystallized in a cubic crystal system with lattice cell pitches $a = 10.685\text{ \AA}$ [2] and is described as a complicated spinel structure with crystal SSG $Fd3m$. Data on phase contents and structures provided in [1–5] refer to bulk samples.

The paper is devoted to electron diffraction investigations of interaction of thin films of Cu_2S and In_2S_3 binary compounds, formation of CuIn_5S_8 ternary compound in a thin-film state and crystallization kinetics mechanism of CuIn_5S_8 amorphous films, that cannot be replaced with other investigations and are important challenges of the modern materials science — development of nanosized semiconductor materials with brand new physical, chemical and other properties. Phase formation processes and structural changes were studied using EMR-102 electron diffractometer. Phase transformations caused by external effects were studied using a kinematic electron diffraction method the use of which leads to qualitative transition from investigations of bulk samples to investigations of ultrathin layers of chemical compounds and their solid solutions in film version. Using the kinematic electron diffraction method that is one of the high-energy electron diffraction (HEED) methods, steady-state activation energies of crystal nucleation and crystal nucleus growth are measured by means of study of time-temperature relationship of amorphous film crystallization. The thin films of interest that are condensed in normal conditions and when exposed to $500\text{ V}\cdot\text{cm}^{-1}$ external electrical field were obtained in a vacuum evaporator combined with UIP-1 universal DC source. Residual gas pressure in the vacuum evaporator was equal to $\leq 10^{-5}\text{ Pa}$

2. Experimental methods

In order to produce nanosized CuIn_5S_8 films and further study them using the HEED method from two independent sources, weighed samples of Cu_2S and In_2S_3 binary compounds on a 1:5 ratio were evaporated. The weighed samples were evaporated from conically wound tungsten coils whose capacity enabled complete and fast evaporation to avoid decomposition and to ensure identical composition of initial phases and deposited thin films. During successive and simultaneous condensation, weighed Cu_2S and In_2S_3 (~ 2.5 and 12 mg, respectively) were put into the evaporation sources spaced at 120 mm. The sources were placed at a height of 70 mm from the substrate planes deaerated in vacuum at 523 K during 2 h. Fresh micron-thick NaCl and KCl single-crystal chips were used as substrates. It is known that component evaporation procedure plays an important role in the phase formation process. Two sets of experiments were carried out. In one case, Cu_2S was evaporated to a In_2S_3 layer preliminary deposited on substrates at room temperature, and in the other case — In_2S_3 was evaporated to Cu_2S . Evaporation was carried out with a rate of $\sim 20\text{--}25$ Å/s.

Since Cu_2S and In_2S_3 differ greatly from each other in the nature of evaporation, simultaneous vapor deposition of these compounds required preliminary study of the evaporation conditions individually for each of them that was necessary to ensure synchronous evaporation. The substances were evaporated from tantalum boats. The preliminary experiments have shown that Cu_2S was quickly and easily evaporated even at very low „boat“ heating current. As opposed to the above substance, In_2S_3 is evaporated in rather peculiar way. In_2S_3 boats melt even at minor heating. A bit higher heating leads to In_2S_3 spreading. In_2S_3 boats evaporate intensively only by means of white heat. Relying on these facts, we carried out simultaneous evaporation of these substances. At first, a boat with In_2S_3 was heated, In_2S_3 melted and wetted the boat walls. At that time heating of Cu_2S boat was started. Evaporation of Cu_2S began almost immediately, at the same time In_2S_3 boat was brought to white heat. The whole process took $\sim 7\text{--}10$ s.

To avoid oxidation and re-evaporation of films during the subsequent heat treatment, the films were placed in carbon capsules, i.e. a version of a film encapsulation method was used that was initially proposed in [6,7]. Analysis of compounds enclosed in a carbon capsule, on the one hand, makes the experiment process more complicated, but on the other hand, it allows to obtain more objective findings: the film encapsulation method needs great care, which, however, makes it possible to minimize the effects with moisture absorption by samples from the ambient air and during heat treatment of samples. The thickness of the films of interest, including carbon ones, did not exceed 500 Å, the alloy system obtained using this method with gradually changing composition contains from 0 to 100%

Cu_2S , from 100 to 0% In_2S_3 on the condensation plane edges.

A normal diffraction pattern of a polycrystalline substance is a series of concentric circles with different intensity. When phase transition kinetics in thin layers is studied, a set of electron diffraction pattern images with different heat treatment could be made on a single photoplate, but these images will be made in some interval of time during which phase changes can take place in the test sample. Therefore, it is necessary to record the diffraction pattern continuously during parallel film heating.

In order to obtain kinematic diffraction images, a diffraction field section on the horizontal diameter was selected from the polycrystalline sample diffraction pattern using a narrow-slot screen. In this case, diffraction images look like a set of short arcs close to straight lines. When the photoplate moves in front of the slot, parallel lines are recorded on it with their position and intensity changing depending on the changes in the substance structure and state. With accelerating voltage 50 kV, the electron diffractometer constant was $2L\lambda = 70.5$ mm · Å.

3. Results and discussion

When investigating the phase interaction and formation processes, in order to obtain films with completely formed structures and strictly stoichiometric ratios, we used a method proposed in [6,7] that enabled control of a geometrically set thickness of the films to be formed. The substance assay, condensate content distribution by coordinates on a unit area of the condensation plane were calculated using the following equation

$$q = \frac{Q}{4\pi h^2} \frac{1}{(1 + \lambda)^{3/2}}. \quad (1)$$

Here, q is a amount of substance on the unit area of the collector, Q is the amount of evaporated substance, h is the distance from the evaporation source to any point on the condensate distribution plane, coefficient $\lambda = x/h$, where x is the distance from the point directly under the evaporator to any point in the distributed condensate over the entire collector area. The film thickness was calculated using the following equation

$$H = \frac{q}{\rho}, \quad (2)$$

where ρ is a substance density in g/cm^3 .

Under simultaneous and layer-by-layer condensation of Cu_2S and In_2S_3 , we have obtained 30 samples independently of the evaporation sequence, and for all of them diffraction pattern images were made. Calculation of diffraction images from the objects obtained using the simultaneous evaporation method has shown that the phase distribution over the condensation plane did not differ from the separate evaporation, i.e. the phase formation pattern was not changed by the interaction reactions —

the composition interval and phase length on the substrates were unchanged. The electron diffraction investigation of films formed during Cu_2S and In_2S_3 vapor deposition on the substrates at room temperature has shown that amorphous films are formed in a wide region on the condensation plane beginning from the substrates located immediately under the In_2S_3 source towards the Cu_2S evaporator. Only one crystalline phase formed on the substrates under the Cu_2S evaporator was observed. Values $\rho = 4\pi \sin \theta / \lambda$ corresponding to diffuse halations observed on the diffraction images obtained from amorphous films formed on the substrates under the In_2S_3 source were equal to 2.211, 3.388, 5.365 \AA^{-1} , and crystallization leads to formation of a cubic structure whose parameters are specified in [5].

Heat treatment of amorphous films with ρ equal to 1.892, 3.094, 4.331 \AA^{-1} located in the center of the condensation plane allowed to find polycrystalline CuIn_5S_8 with pitches specified in [2]. The phase distribution diagram based on the electron diffraction analysis of the films obtained from the NaCl and KCl single-crystal substrates spaced at 3 mm with the total condensation length 120 mm has shown that distinct interfaces between the amorphous films and films formed in crystalline state were observed in all cases notwithstanding the method used.

Kinematic diffraction pattern images from amorphous films crystallized in a CuIn_5S_8 cubic crystal system, where both phase (amorphous and crystalline) regions were observed and changes in the diffraction line intensities of the growing crystalline phase corresponding to different time points were obtained at 403, 418, 433 K. Figure 1 shows a kinematic diffraction pattern image made at 418 K.

A threshold temperature for amorphous CuIn_5S_8 was equal to 458 K at which immediate crystallization of the amorphous film took place and this prevented from tracing the entire phase transition behavior. Diffraction lines on the kinematic diffraction pattern image from a polycrystal are indicated based on the pitches specified in [2]. As shown on the kinematic diffraction image, increase of diffraction line intensities from the crystalline phase with time during crystallization was due to the increase of the amount of polycrystalline phase exposed to the electron beam, i.e. variation of diffraction line intensities of one phase is associated with the variation of the amount of this phase in the irradiated volume, since the total amount of the substance remains unchanged. Since a small section from the diffraction pattern (DP) is recorded on the kinematic diffraction image, the local intensity of Debye ring according to [8] is expressed by the following equation

$$I_{hkl} = I_0 \lambda \left[\frac{\Phi_{hkl}}{\Omega} \right]^2 V \frac{d_{hkl} \Delta P}{4\pi L \lambda}. \quad (3)$$

here, I_0 is the initial electron emission beam intensity, λ is the electron wave length, Φ is the structural diffraction reflection amplitude that is calculated from atomic scattering factors in kinematic approximation, Ω is the lattice cell

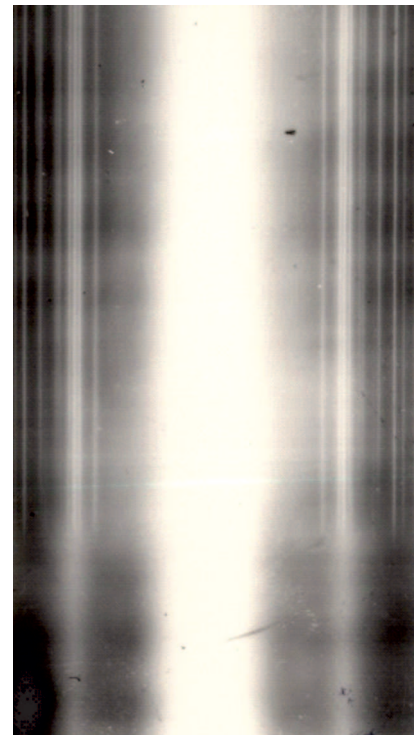


Figure 1. Kinematic diffraction pattern image from amorphous CuIn_5S_8 undergoing phase transformation at 418 K.

volume, V is the irradiated polycrystalline preparation volume, d_{hkl} and Δ is the interplanar spacing and small Debye ring area, respectively, P is the diffraction reflection gain multiplicity factor, $L\lambda$ is the instrument constant depending on the applied voltage that accelerates electrons.

During kinematic imaging, the values included in the right-hand side of equation (3) remain constant, except for V . The diffraction reflection intensity with indices hkl provided that I_0 and $L\lambda$ are constant as specified in (8) is proportional to the irradiated polycrystalline substance volume, i.e. $I_{hkl} \sim V$. Thus, when the changed diffraction line intensity has been determined using the kinematic diffraction images, changes in the amount of substance undergoing phase transformation may be found. A completely crystallized volume — $S \cdot h$ was matched with its corresponding maximum intensity obtained during saturation, where S is the cross-section area of the electron beam equal to $\sim 2.8 \cdot 10^{-3} \text{ cm}^2$, h is the film thickness equal to 250 \AA .

Microphotomatering of various areas on the kinematic diffraction images depending on the film heat treatment time was used to define the DP line intensity with indices (220), (320) and (402). The volumes of the crystallized portion of CuIn_5S_8 determined using the specified diffraction reflections are much the same, with the threshold values equal to:

$$V = S \cdot h = 8 \cdot 10^3 \text{ cm}^2 \cdot 2.5 \cdot 10^{-6} \text{ cm} = 7 \cdot 10^{-9} \text{ cm}^3.$$

The obtained value also matches the value found from the following arguments: since the electron beam radius

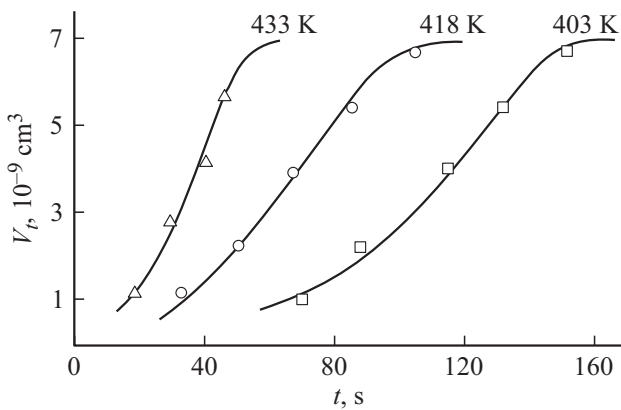


Figure 2. Kinetic crystallization curves of amorphous CuIn_5S_8 .

is 0.3 mm ($S = 2.8 \cdot 10^{-3} \text{ cm}^2 = \pi r^2$, $r = \sqrt{(28 \cdot 10^{-4})/\pi} = 3 \cdot 10^{-2} \text{ cm}$), then $V = \pi r^2 h = S \cdot h = (2.8 \cdot 10^{-3} \text{ cm}^2) \times 2.5 \cdot 10^{-6} \text{ cm} = 7 \cdot 10^{-9} \text{ cm}^3$.

Figure 2 shows the volume of the crystallized portion of CuIn_5S_8 vs. the annealing time at 403, 418, 433 K, i.e. kinetic crystallization curves of amorphous CuIn_5S_8 that crystallize in the cubic crystal system.

The analytic expression describing kinetic patterns of phase transformations was obtained in [9] as the following equation

$$V_t = V_0[1 - \exp(-kt^m)]. \quad (4)$$

Here, V_t is the crystallized substance volume by the time t , V_0 is the initial volume, k is the reaction rate constant equal to $\frac{1}{3} \pi v_3 v_p^3$, where v_3 and v_p are the nucleating seed formation and further growth rates, respectively, that are described by the following expressions

$$v_3 = A_1 \exp\left(-\frac{E_3}{RT}\right), \quad v_p = A_2 \exp\left(-\frac{E_p}{RT}\right),$$

where A_1 and A_2 are some temperature-independent constants, E_3 and E_p are crystal nucleation and growth energies, respectively, R is the universal gas constant, T is the absolute temperature. Value m is different for possible types of transformations and depends on the crystal growth rhythm.

To compare the isotherm curves with equation (4) that enables to define the phase transformation kinetics pattern, this analytical equation may be represented as follows

$$\ln \ln \frac{V_0}{V_0 - V_t} = \ln k + m \ln t. \quad (5)$$

Using the experimental data for the above temperatures, $\ln \ln \frac{V_0}{V_0 - V_t}$ vs. $\ln t$ curves were plotted (Fig. 3), where the experimentally found points for all three temperatures fall on straight lines indicating that the experimental isotherms are well described by the expression established by Avrami–Kolmogorov. From the slope of straight lines to X axis shown in Fig. 3, the found values for exponent t were

equal to ~ 4 ($m = 3.88$ for 433 K, $m = 3.91$ for 418 K, $m = 3.97$ for 403 K).

Thus, the comparison of the experimental isotherms with the analytical expression has shown that the best coincidence takes place at $m \approx 4$. This value found for m shows that a three-dimensional growth of crystals takes place in case of crystallization of amorphous CuIn_5S_8 films. According to (5), intersection of $\ln \ln \frac{V_0}{V_0 - V_t}$ vs. $\ln t$ dependence lines with Y axis is defined by $\ln k$. $\ln k$ obtained for the above temperatures were as follows: at 403 K $\ln k = -25.4$, at 418 K $\ln k = -19.7$, at 433 K $\ln k = -15.5$. By the slope of $\ln k$ vs. reciprocal temperature line, total crystallization energy of amorphous CuIn_5S_8 was defined and included two summands: $E_{\text{sum}} = E_3 + E_p$. It is equal to 75.9 kcal/mole. The crystal nucleation rate is adequately described by the reciprocal incubation time $1/\tau_0$, i.e. is characterized as $E_3 \sim 1/\tau_0$. The nucleation activation energy calculated using the slope of $\ln 1/\tau_0$ vs. reciprocal temperature line was equal to 23.2 kcal/mole. The crystal growth activation energy defined from $E_p = (E_{\text{sum}} - E_3)/3$ is equal to 17.6 kcal/mole.

The crystallization kinetics of amorphous CuIn_5S_8 films deposited under the external electrical field exposure was investigated in the similar way as for the films condensed in normal conditions. In this case, for crystallization of thin amorphous CuIn_5S_8 layers at all test temperatures in the range of 403–433 K more time is required for crystallization of films formed outside the field. The total crystallization activation energy (E_{sum}) for the films to be formed under the electrical field exposure, nucleation activation (E_3) and growth (E_p) energies were defined similarly to the case without the electrical field and were equal to 88.5, 26.7, 20.6 kcal/mole, respectively, they were greater than the corresponding values for films formed in normal conditions: amorphous CuIn_5S_8 layers formed under the electrical field exposure are more stable than without the electrical field.

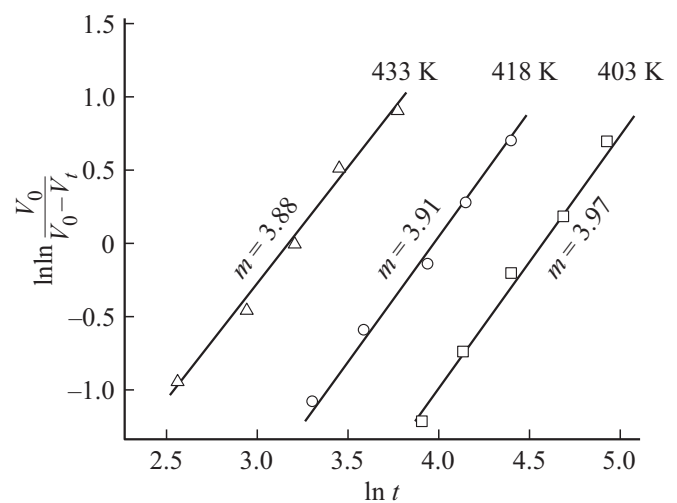


Figure 3. Dependence $\ln \ln \frac{V_0}{V_0 - V_t}$ from $\ln t$ for crystallization of amorphous CuIn_5S_8 .

4. Conclusion

During simultaneous and layer-by-layer depositions of Cu_2S and In_2S_3 regardless of the evaporation sequence, composition interval and phase length on the condensation plane, amorphous phases of In_2S_3 and CuIn_5S_8 compounds and one crystalline phase of Cu_2S compound are formed and remain unchanged.

Crystallization kinetics of amorphous CuIn_5S_8 films formed by means of Cu_2S and In_2S_3 molecular beam deposition in normal conditions and under exposure to $500 \text{ V} \cdot \text{cm}^{-1}$ electrical field is governed by the patterns established by Avrami–Kolmogorov and is described by expression $V_t = V_0[1 - \exp(-kt^m)]$. In amorphous films, three-dimensional crystal growth takes place during crystallization. Nucleation activation and crystal growth energies for the films formed under the electrical field exposure are greater than that for the films formed outside the electrical field by $\sim 15\%$.

Conflict of interest

The authors declare that they have no conflict of interest.

References

- [1] I.V. Bodnar, M.A. Zhafar. Dokl. BGUIR, **5** (107), 40 (2017) (in Russian).
- [2] S. Kitamura, S. Endo, T. Irie. J. Phys. Chem. Solids, **8** (46), 881 (1985).
- [3] N.S. Orlova, I.V. Bodnar, E.A. Kudritskaya. Neorg. mater., **8** (33), 932 (1997) (in Russian).
- [4] I.V. Bodnar. FTP, **32** (9), 1043 (1998) (in Russian).
- [5] M. Hansen, K. Anderko. *Struktura dvoynykh splavov* (M., Metallurgizdat, 1962) V. 2, p. 1488 (in Russian).
- [6] E.B. Askerov, A.I. Madadzada, D.I. Ismailov, R.N. Mekhtieva. FTP, **48** (9), 1265 (2014) (in Russian).
- [7] E.B. Askerov, A.I. Madadzada, D.I. Ismailov, R.N. Mekhtieva. FTP, **48** (11), 1484 (2014) (in Russian).
- [8] B.K. Vainshtein. *Structurnaya electronographiya* (M., Isd-vo AN SSSR, 1956) p. 313 (in Russian).
- [9] M. Avrami. J. Chem. Phys., **8** (2), 212 (1940).